Boletín Geológico

SERVICIO GEOLÓGICO COLOMBIANO

Boletín Geológico, 51(1), 2024

https://doi.org/10.32685/0120-1425/bol.geol.51.1.2024.672

Manuscrito recibido: Agosto 31, 2022

Revisión recibida: Febrero 13, 2024

Aceptado: Febrero 23, 2024

Publicado en línea: Marzo 7, 2024

Research article

Velocity field for Western Venezuela: Elastic modeling in the Southern Merida Andes

Campo de Velocidad para el Occidente de Venezuela: Modelado elástico en la región meridional de los Andes de Mérida

Carlos E. Reinoza[1,2]✉, Franck A. Audemard M.[3,4,5]✉, Ruy Pereira[6]✉, Lenín Ortega[7]✉, Michael Schmitz[2]✉, Luis A. Yegres[1,2]✉, Héctor Mora-Páez[8]✉

[1]Departamento de Sismología, División de Ciencias de la Tierra, Centro de Investigación Científica y de Educación Superior de Ensenada, Baja California, México. reinoza@cicese.mx
[2]Departamento de Geofísica, Fundación Venezolana de Investigaciones Sismológicas, Caracas, Venezuela.
[3]Departamento de Geología, Escuela de Geología, Minas y Geofísica, Facultad de Ingeniería, Universidad Central de Venezuela, Caracas, Venezuela.
[4]División de Ciencias de la Tierra, Centro de Investigación Científica y de Educación Superior de Ensenada, Baja California, México.
[5]Departamento de Ciencias de la Tierra, Fundación Venezolana de Investigaciones Sismológicas, Caracas, Venezuela.
[6]Departamento de Ingeniería Geodésica y Agrimensura, Escuela de Ingeniería Civil, Facultad de Ingeniería, Universidad Central de Venezuela, Caracas, Venezuela.
[7]Petróleos de Venezuela, S.A., Intevep-Los Teques, Venezuela.
[8]Consultor, Bogotá, Colombia.

Abstract

We show new geodetic velocity field for Western Venezuela based on repeated GNSS campaign measurements in 2011, 2013, and 2016. The 28 sites are distributed on the northern side of the Oca-Ancon fault, the eastern Maracaibo Block, and vicinities to the whole extension of the Boconó fault but particularly densified across the La Grita segment in the Southern Mérida Andes. Deformation in western Venezuela based on geodetic measurements has been the object of recent studies, however this contribution focuses on the Southern Merida Andes. We assess the simple homogeneous model for one fault (across La Grita segment of the Boconó fault) and two-faults (Boconó fault and a secondary system) model. Our preferred model of both approaches shows a far-field velocity of 11.3 mm yr^{-1} and a 9.6 km locking depth for the Boconó fault. Nonetheless, the best fit concerning the two-fault model shows a slip rate of 9.5 mm yr^{-1} for the Boconó fault and 1.3 mm yr^{-1} for the Caparo fault. We confirm that the Boconó fault is the main structure that accommodates most of the right-lateral slip between the Maracaibo block and South American plate. A complimentary comparison with the surface velocity model VEMOS17 indicates the need of densifying observation sites through measurement campaigns and continuous GNSS stations. These stations will improve our knowledge of local and regional geodynamics and their implications for seismic hazard studies.

Keywords: GNSS, Tectonic deformation, Fault slip rates, Locking depth, Boconó fault, Caparo fault.

Resumen

En el presente trabajo se presenta un nuevo campo geodésico para el Occidente de Venezuela basado en repetición de mediciones GNSS llevadas a cabo en 2011, 2013 y 2016. Los 28 sitios están localizados al norte de la falla Oca-Ancón, la parte este del Bloque de Maracaibo, y a lo largo de toda la extensión de la Falla de Boconó. El análisis de la deformación basada en mediciones geodésicas ha sido objeto de estudio recientemente. Específicamente, nos enfocamos en la región meridional de los Andes de Mérida. Evaluamos modelos simples homogéneos para una falla (Segmento La Grita de la Falla de Boconó) y para el caso de dos fallas considerando la mencionada falla y la falla Caparo. El modelo preferido considera una sola falla con una velocidad a lo largo de la dislocación de 11.3 mm a^{-1} y 9.6 km de profundidad de bloqueo. Para el caso del modelo de dos fallas, el mejor modelo muestra valores de velocidad de campo lejano de 9.5 mm yr^{-1} para la falla de Boconó y 1.3 mm a^{-1} para la falla de Caparo. Se confirma que la falla de Boconó es la principal estructura que acomoda la mayoría del movimiento lateral derecho entre la placa Sudamericana y el bloque de Maracaibo. Se incluye además una comparación de nuestros resultados con el modelo de velocidad de superficie VEMOS17, que muestra la necesidad de densificar los sitios de observación a través de ocupaciones temporales y de la instalación de estaciones geodésicas de monitorio continuo. Estas estaciones mejorarán nuestro conocimiento sobre la geodinámica local y regional, y sus implicaciones para estudios de amenaza sísmica.

Palabras clave: GNSS, Deformación tectónica, Tasa de deslizamiento de fallas, Profundidad de bloqueo, falla de Boconó, falla de Caparo.

Citación: Reinoza, C.E., Audemard M., F.A. Pereira, R., Ortega, l. Schmitz, M., Yegres, L.A. and Mora-Paéz, H. (2024). Velocity field for Western Venezuela: Elastic modeling in the Southern Mérida Andes. Boletín Geológico, 51(1). https://doi.org/10.32685/0120-1425/bol.geol.51.1.2024.672

1. INTRODUCCIÓN

In western Venezuela, the plate boundary between the Caribbean and South American plates covers an around 600 km wide zone from the Southern Caribbean deformed belt to the Mérida Andes (Silver et al., 1975; Ladd et al., 1984; Audemard, 1993, 1998, 2009; Audemard and Audemard, 2002), which is a prominent mountain range that extends in a SW-NE direction for some 350 km from the Colombian-Venezuelan border in the southwest to the city of Barquisimeto in the northeast with a maximal elevation of 4,978 m a.s.l at Pico Bolívar. The western area comprises a set of discrete tectonic blocks or microplates such as Maracaibo, Bonaire, and North Andean blocks (Figure 1), which move independently among the surrounding larger plates (Caribbean, South America, and Nazca).

This area shows intense deformation and active faults; among them, we can mention the Oca-Ancon fault zone, a right-lateral strike-slip fault system that cuts across the northwestern margin of South America and forms the westernmost strand of a subparallel zone of right-lateral strike-slip faults that includes the San Sebastian and El Pilar fault zones (Audemard, 2000). Another major structure is the Boconó fault, a NE-SW trending fault that extends for about 500 km from the border between Colombia and Venezuela to the Caribbean coast. The main trace of the Boconó fault is interpreted as a take-off surface detaching from the interface between the upper and lower crust and dipping to the SE (Audemard and Audemard, 2002; Avila-García et al., 2022). On the Colombian side, the left-lateral strike slip Santa Marta-Bucaramanga fault bounds the Maracaibo Block to the southwest, which impacts this region's geodynamics.

The shape of western Venezuela largely results from the interaction of the Caribbean and South American plates. According to the geodetic observations north of the Leeward Antilles, the Caribbean plate subducts the South American plate characterized by an oblique convergence (Pérez et al., 2001a; Weber et al., 2001; Trenkamp et al., 2002; Pérez et al., 2011). Some authors mention that this north-south convergence took place along a very low angle subduction offshore of the Santa Marta Massif to dip steeply to the ESE under the Mérida Andes (Kellogg, 1984; Van der Hilst and Mann, 1994; Malavé and Suárez 1995; Taboada et al. 2000; Colmenares and Zoback, 2003; Dhont et al., 2005; Backé et al., 2006; Bezada et al., 2010).

This North-South shortening has been attributed to north-south Cenozoic convergence between the North and South American plates (e.g., Pindell and Dewey 1982; Audemard, 1993, 1998, 2009; Colmenares and Zoback 2003) suggesting a period of particularly fast convergence (~10 mm/yr^{-1}) that likely began in the early Miocene and continues to the present-day (Kellogg, 1984). Pindell and Barrett (1990) suggest a 250–300 km north-northwest–directed convergence between North and South America since the middle Eocene. Conversely, Müller et al. (1999) described several phases of northeast-southwest oriented convergence from the early Eocene until chron 18 (38.4 Ma). Jarrin et al. (2023) recently confirmed that slow active subduction is decreasing eastward along the Southern Caribbean Deformation Belt. The rates vary from ~4.5 mm yr^{-1} in Colombia to ~1-2 mm yr^{-1} in offshore northern Venezuela. These results are consistent with a low-angle subduction interface, initially proposed by Van der Hilst and Mann (1994), with no relevant interseismic coupling.

From a wider perspective, the Pliocene to Holocene subduction of the Nazca plate in western South America and the collision of the Panamá Arc with western Colombia are responsible for the east-west plate convergence (Kellogg, 1984; Mann et al., 1984; Trenkamp et al., 1995). Many authors have related the collision of the Panamá Arc to the northward extrusion or escape of continental fragments (The Maracaibo block, the northern Andes and the Bonaire block) in a north-to-northeasterly direction (Pennington, 1981; Mann et al., 1984, 1991; Stephan et al., 1990; Audemard, 1993, 1998, 2009, 2014a; Van der Hilst and Mann, 1994; Trenkamp et al., 1995; Egbue and Kellogg, 2010).

From stratigraphic and paleontological studies, authors infer that the collision between Panamá and South America started at 10 Ma (Duque-Caro, 1979; Coates et al., 2004). Other authors propose an effective later suturing date of about 5 Ma (Audemard 1993, 1998, 2009, 2014b; Audemard and Audemard, 2002; Audemard et al., 2005). The absence of volcanism in Western Venezuela could be related to the shallow dip of subduction as has been reported in Peru and Chile, where effectively no asthenospheric wedge exists to produce source material for volcanism (McGeary et al., 1985; Gutscher et al., 2000).

An overview from the west shows that the Eastern Cordillera extends northward into the Mérida Andes and the Perijá Range, spreading across the Venezuelan-Colombian border and the Santa Marta block in Colombia. The uplift of the Eastern Cordillera is likely related to flat-slab subduction of the southern edge of the Caribbean plate under the northern South American plate (Kellogg and Bonini, 1982; Bezada et al., 2010). Nonetheless, the timing of the uplift is generally related to the Panamá Arc-South America collision (Molnar and Sykes, 1969).

Audemard and Audemard (2002) propose a Pliocene-Quaternary transpression due to oblique convergence between the South American plate and Maracaibo block to explain the Mérida Andes buildup, also known as Venezuelan Andes. The strain partitioning along the chain is taken by across shortening by the

foothills and the mountain belt buildup in a NW-SE direction, while the Boconó Fault accommodates along-chain dextral slip.

Concerning the object of this study, GNSS measurements provide accurate data on tectonic displacements and allow for determining the geodetic velocity fields in a short period. Western Venezuela was part of the first civil efforts to establish a GPS Network, the CASA UNO Project (UNO in Spanish to designate the first epoch of measurements) in 1988 (Kellogg and Dixon, 1990). Five stations were occupied in this first campaign between January and February 1988. Later, the Venezuelan network increased to 21 stations covering the western and eastern parts of the country. Since 1994, several campaigns of GPS measurements have been headed by a working group comprising national and international institutions: the University Simón Bolívar (USB), University of Colorado (UC), National Cartography Institute (now Simón Bolívar Geographical Institute of Venezuela -IGVSB) and University of Zulia (LUZ) with remarkable results (Pérez et al., 2001a, 2001b, 2011, 2018). In late 2011, 19 new brass rock outcrop-glued sites were installed by the Venezuelan Foundation for Seismological Research (FUNVISIS) (Figure 1).

Late the same year, this Venezuelan institution, with the support of Petroleum of Venezuela, S.A. (PDVSA), and IGVSB, measured 30 sites, including some of the newly installed sites during this 2011 measuring campaign. In early 2013, 26 sites were reoccupied (Reinoza, 2014). As part of a new campaign, between January 18 and February 5, 2016, 33 sites were reoccupied (Molero, 2020). The monumentation performed since 2003 by FUNVISIS introduce two new aspects: a) brass spits are glued to stable bedrock outcrops or existing concrete benchmarks from other institutions (IGVSB, UNAVCO, among others; Jouanne et al., 2011), suppressing the sensitive use of tripods since antennas are directly screwed to bedrock with brass rods or extensions; b) The geographic spreading of the spits responds to two scientific aims: 1) slip rate of individual faults, regardless of their seismogenic potential and 2) tectonic rotation of discrete tectonic blocks (Reinoza, 2015; Audemard et al., 2020).

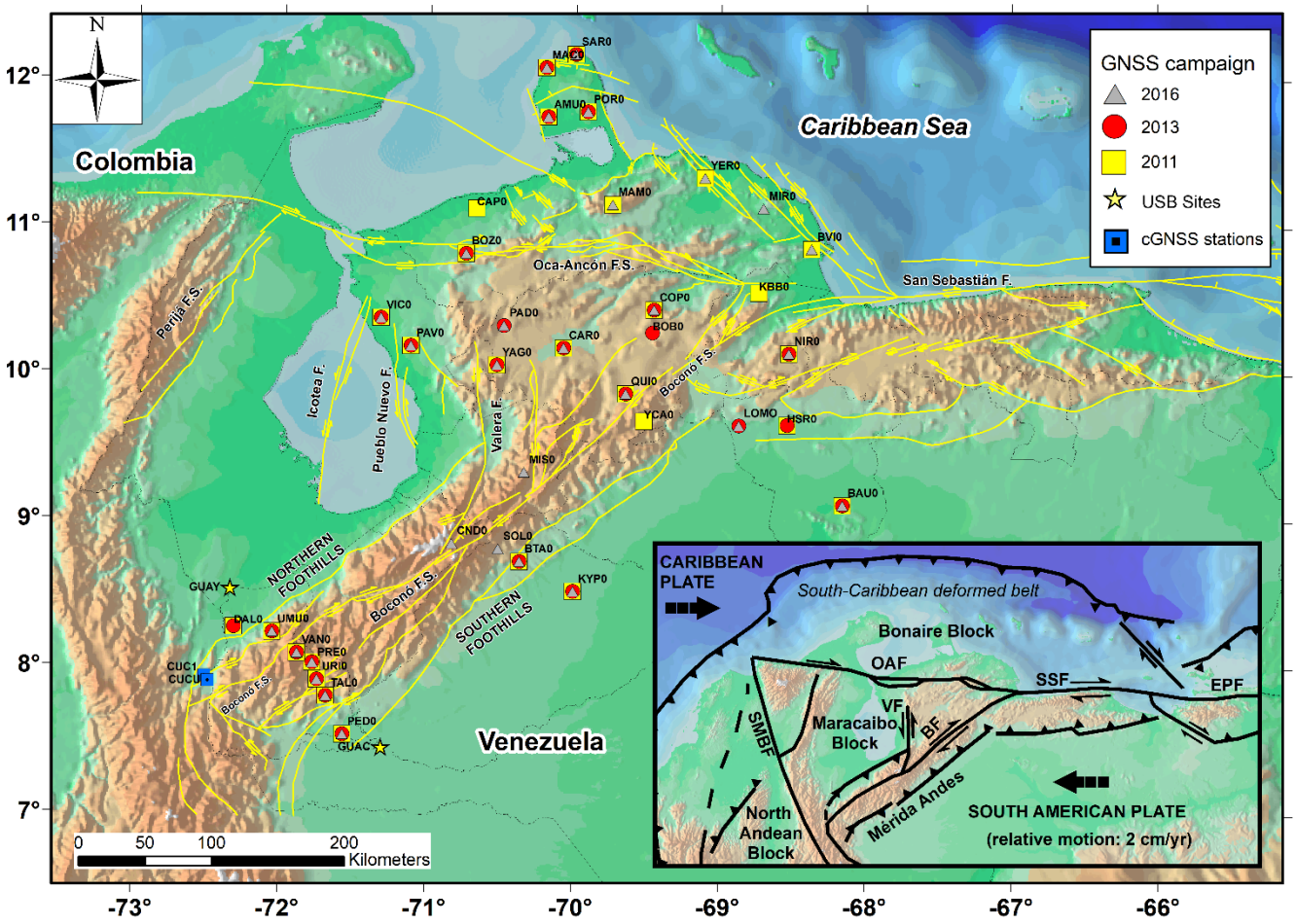

Figure 1. Distribution of 2011, 2013, and 2016 campaign sites, Universidad Simón Bolívar Network campaign sites (Pérez et al., 2018), and cGNSS sites in Colombia territory. The map of active faults in Venezuela is from Audemard et al. (2000). The inset box shows a schematic geodynamic map of the southeastern Caribbean margin (Audemard et al., 2000; Trenkamp et al., 2002).

Deformation in western Venezuela based on geodetic measurements has been the object of recent studies. From elastic models from early GPS measurements, Pérez et al. (2001b) determine 9-11 mm yr^{-1} of dextral shear and 1 mm yr^{-1} of convergence on the Boconó fault. Later, Pérez et al. (2011) carried out GNSS measurements in western Venezuela, emphasizing on the Venezuela Andes. These observations revealed that the 20 ± 2 mm yr^{-1} of eastward displacement of the Caribbean plate relative to the South America plate is partitioned into 12 ± 2 mm yr-1 of right lateral displacement on the Boconó Fault and a normal convergence of 12-16 mm yr^{-1}, where almost a 1/3 concentrates in the Andean region close to the Boconó fault. They indicate the fault segment is almost vertical with a 14 ± 4 km locking depth. Symithe et al. (2015) included the Maracaibo and the North Venezuela (NVEN) blocks to evaluate the contribution of western Venezuela as part of the kinematic block model for the Caribbean.

The Maracaibo block is delimited by the Boconó, Santa Marta-Bucaramanga, and Oca-Ancón faults (e.g., Audemard et al., 2000; Audemard and Audemard, 2002; Audemard, 2009, 2014a). Symithe et al. (2015) assigned a clockwise rotation of 0.635 ± 0.180° Ma-1 relative to the North American Plate. The NVEN block, related to the Bonaire Block and part of the Southern Caribbean deformation belt, yielded a similar rotation of 0.687 ± 0.194° Ma-1 relative to the North American plate. Pérez et al. (2018) recently performed kinematic block modeling that included the North Andean block and the Caribbean-South America plate margin. This study shows two models as best fits (Models 4 and 5 in the quoted manuscript); the first model considers the Maracaibo and Bonaire blocks as one unit with a rotation rate of 0.403 ± 0.135° Ma-1 relative to the South American plate.

The second model comprises the Maracaibo blocks (0.660 ± 0.080 ° Ma-1), but the South Caribbean Deformed Belt is split into western (0.603 ± 0.079° Ma-1) and eastern (0.341 ± 0.322° Ma-1) sections; all rates are relatives to the South American plate. For this study, the authors keep the known value of ~9 and 11 mm yr^{-1} of dextral shear (Perez et al., 2001b) for the Boconó fault but fix 2-5 mm yr^{-1} of convergence across adjacent and subparallel thrust faults. Lizarazo et al. (2021) recently reported a new tectonic model for Northern Colombia, including part of northwestern Venezuela. They proposed a new block named "Macondo," which comprises the septentrional part of the North Andean block and the whole Maracaibo and Bonaire blocks. This conception is clearly incompatible with the most known models, consisting of two geologically defined blocks (Maracaibo and Bonaire) for northwestern Venezuela (Audemard, 2014a). Mogollón-López et al. (2019), from data acquisition campaigns, carried out in 2011, 2013, and 2016 (Reinoza, 2014; Molero, 2020), applied different modeling approaches: (1) simple-homogeneous and asymmetric elastic models for the Oca-Ancón fault; (2) a two-fault model that includes the Oca-Ancón fault and the northernmost sections of the Boconó fault; and (3) a simple-homogeneous elastic model for the northern area of the Boconó fault.

The best models indicated a far-field velocity of 1.50 ± 0.05 mm yr^{-1} and a locking depth of 16.5 ± 3 km for the Oca-Ancón fault. They determined a velocity of 15-16 mm yr^{-1} with a locking depth of 12 km for the northeast segments of the Boconó fault (Guarico and San Felipe segments, Audemard, 2014b) From these results, the authors concluded that the Oca-Ancón fault system accommodates approximately 7-8 percent of the right lateral displacement between the Caribbean and South American plates, and the Boconó fault accommodates approximately 80 percent of the 20 mm yr^{-1}. These results were consistent with two Pleistocene rates for the Boconó fault (Yaracuy Valley) of < 20 mm yr^{-1} and 5.0-11.2 mm yr^{-1} based on 10Be cosmogenic dating and measurement of tectonic displacement on high-resolution satellite images (Pousse-Beltran et al., 2017).

Here, we present a new velocity field of Western Venezuela in the ITRF2014 reference frame (Altamimi et al., 2017) based on 2011, 2013, and 2016 GNSS data. We include a comparison with the velocity model VEMOS17 (Drewes and Sánchez, 2020). Next, we focus on the Southern region of the Merida Andes, assessing a simple homogeneous model for one fault (The southern part of the Boconó fault) and two faults (the Boconó and Caparo faults) model. This region comprises a complex deformation zone dominated by the Boconó fault and other secondary strike-slip faults and thrust in the northwest flank. This region has been affected by the historical 1610, 1644, 1849, 1875, 1894, and 1932 earthquakes (Ramírez, 1953; Palme et al., 2005; Cifuentes and Sarabia, 2007; Galán and Casallas, 2010; Palme et al. 2012; Salcedo-Hurtado et al., 2021) (Figure 2).

2. GNSS DATA COLLECTION

The observation at 28 sites located in western Venezuela in successive campaigns in 2011, 2013, and 2016 was performed with GPS/GNSS double-frequency receivers and geodetic antennas for at least 48 hours and up to 120 hours (5 days) with a 30-second sampling rate (Reinoza, 2015). The Bernese 5.2 software (Dach et al., 2015) was used to provide a new solution in the ITRF2014 reference frame following a double-difference strategy described in previous studies (Jouanne et al., 2011; Reinoza et al., 2015; Ávila-Barrientos et al., 2021). The IGS (International GNSS

Service) sites used as reference sites are BOGT, BRAZ, BRFT, BRMU, CRO1, GUAT, and SCUB (Table 1).

The Bernese software underestimates the daily coordinate errors because of systematic errors or mismodeled parameters that are not included in the formal error (Hugentobler et al., 2001). To obtain a realistic estimated error, we rescaled the formal velocity errors, multiplying them by a factor of 10. Although ITRF2014 introduces an innovation by correcting the Post-Seismic Deformation (PSD), we select only reference stations without PSD corrections to derive linear velocities from our series of normal daily equations (Dach and Fridez, 2019). Figure 3 shows the GNSS time series position for the 22 sites occupied during all three campaigns. All sites show linear trends without perturbations such as coseismic jumps, landslides, or human-induced errors.

Also, we show velocities expressed in the ITRF2014 Reference Frame (Figure 4; Table 2) and the South America Plate Reference frames (Figure 5).To complement the Southern Andes model analysis, we included data from continuous geodetic stations: CUC1 (Colombian Geological Survey –SGC/GeoRED) and CUCU (Geographic Institute Agustin Codazzi –IGAC/Francisco de Paula Santander University –UFPS). Also, we consider the velocity result from GUAY and GUAC sites obtained by Pérez et al. (2018).

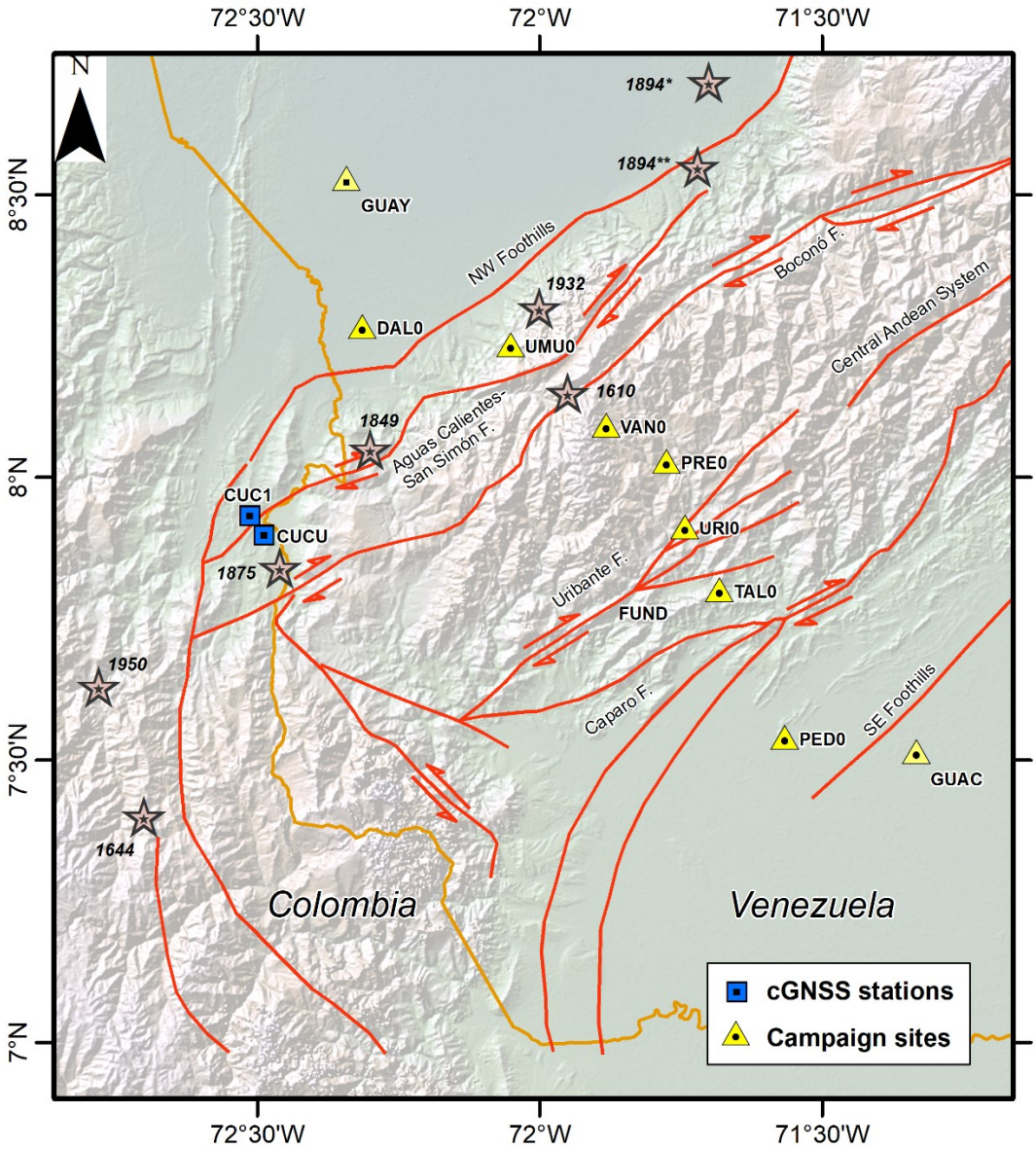

Figure 2. Campaign GNSS sites in the Southern Merida Andes. Quaternary fault map from Singer and Beltran (1996) and Audemard et al. (2000). Rose stars represent this region's main destructive seismic event epicenters. 1610: Ml 7 (Palme et al., 2012); 1644: Mw 6.9 (Cifuentes and Sarabia, 2007) ; 1849: Mw 6.3 (Palme et al., 2005) ;1875: Mw 6.75 (Galan et al., 2016) ; 1894*: Mw 7.5 (Palme et al., 2005); 1894**: Mw 7.63 (Salcedo-Hurtado et al., 2021); 1932: Mw 6.5 (Palme et al., 2005); 1950: Ml 7 (Ramírez, 1953).

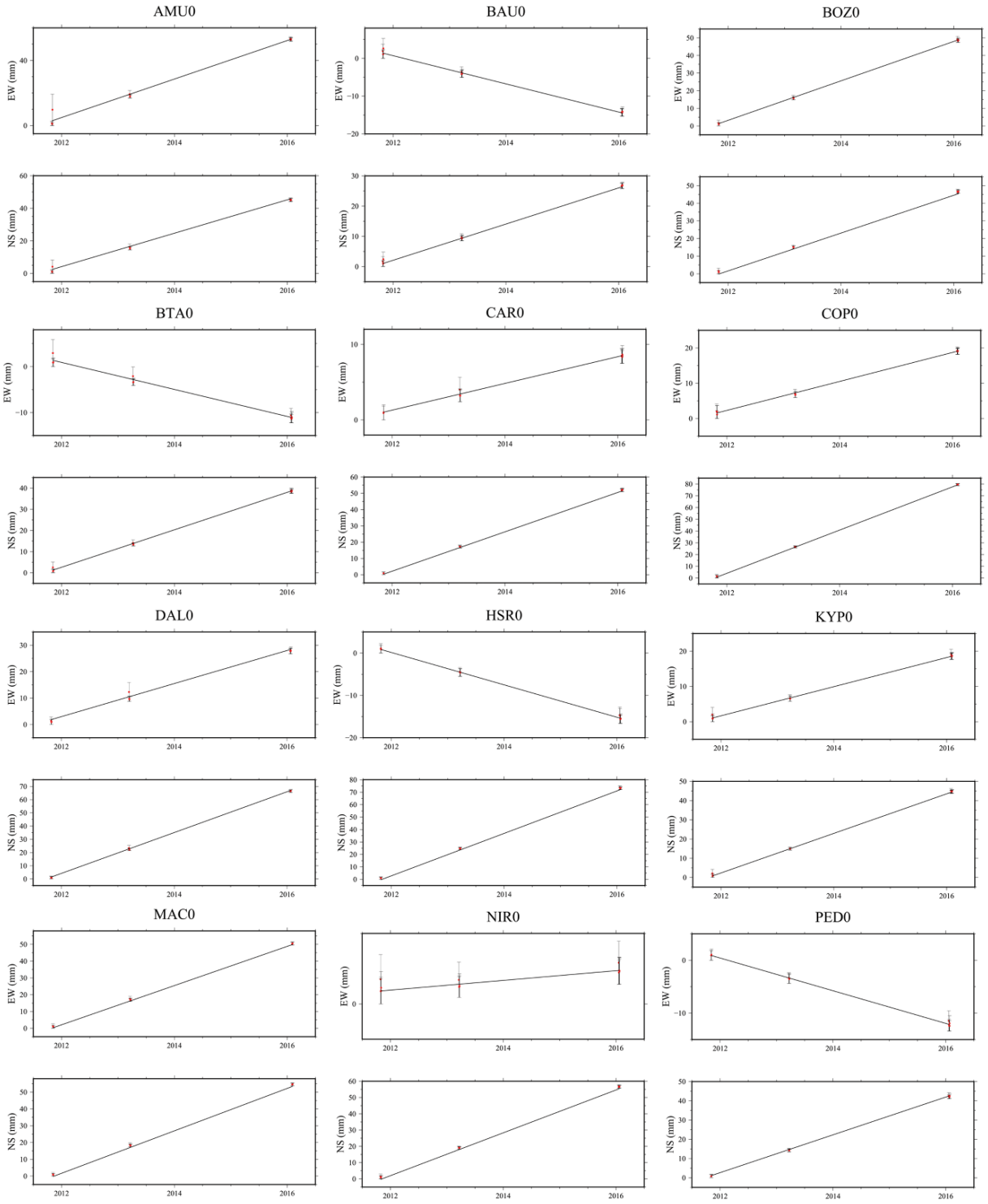

Figura 3. GNSS time series position for all sites occupied during all campaigns (2011, 2013, and 2016). The trendline is calculated using NS and EW (mm) velocities expressed in the ITRF2014 Reference Frame.

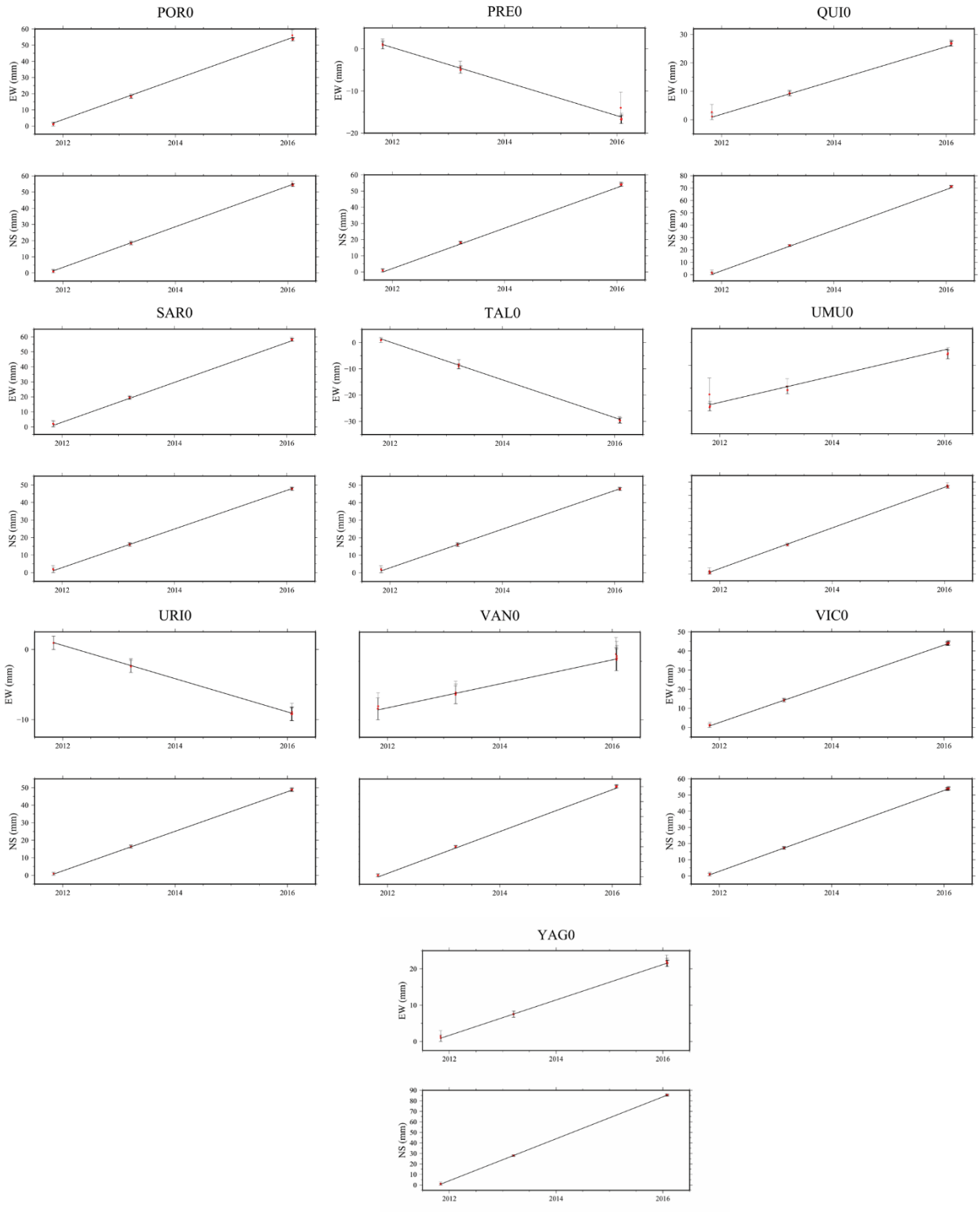

Figure 3. (Continued) GNSS time series position for all sites occupied during all campaigns (2011, 2013, and 2016). The trendline is calculated using NS and EW (mm) velocities expressed in the ITRF2014 Reference Frame.

Table 1. IGS sites used as reference stations (Johnston et al., 2017)

Site ID	Long (deg)	Lat (deg)	Height (m)	Country	Tectonic Plate	Operational Status
BOGT	4.640	-74.081	2577.179	Colombia	South American	Active
BRAZ	-15.947	-47.878	1106.445	Brazil	South American	Active
BRFT	-3.877	-38.426	22.074	Brazil	South American	Active
BRMU	32.370	-64.696	-11.610	UK	North American	Retired
CRO1	17.757	-64.584	-31.092	Virgin Islands (U.S.)	Caribbean	Active
GUAT	14.590	-90.520	1520.277	Guatemala	Caribbean	Active
SCUB	20.012	-75.762	21.436	Cuba	North American	Active

Table 2. Velocities Expressed in the ITRF2014 Reference Frame

Site ID	Long (deg)	Lat (deg)	Ve (mm yr^{-1})	Vn (mm yr^{-1})	σVe (mm yr^{-1})	σVn (mm yr^{-1})	Speed (mm yr^{-1})
AMU0	-70.188	11.753	12.3	10.4	1.3	1.1	16.1
BAU0	-68.158	9.118	-3.6	6.1	1.3	1.2	7.1
BOZ0	-70.746	10.819	11.2	10.7	1.2	1.1	15.5
BTA0	-70.367	8.726	-2.9	8.9	1.2	1.1	9.3
BVI0	-68.374	10.861	12.5	13.4	1.6	1.3	18.3
CAR0	-70.066	10.177	1.8	12.1	1.1	1.0	12.2
COP0	-69.454	10.442	4.3	18.4	1.2	1.0	18.9
CUC1*	-72.513	7.932	6.6	13.2	0.8	0.7	14.8
CUCU*	-72.488	7.898	4.8	15.2	0.8	0.7	15.9
DAL0	-72.314	8.267	6.3	15.5	1.3	1.1	16.7
HSR0	-68.538	9.661	-3.9	17.0	1.3	1.2	17.4
KYP0	-69.999	8.524	4.2	10.3	1.1	1.0	11.1
LOM0	-68.870	9.658	7.4	17.7	1.6	1.4	19.2
MAC0	-70.204	12.089	11.7	12.7	1.2	1.0	17.2
MAM0	-69.743	11.158	8.7	11.7	1.4	1.2	14.6
NIR0	-68.536	10.152	0.3	13.2	1.1	0.9	13.2
PAD0	-70.483	10.331	5.3	19.4	2.0	1.5	20.1
PAV0	-71.120	10.189	10.2	6.8	3.8	3.1	12.2
PED0	-71.566	7.540	-3.2	9.8	1.3	1.1	10.3
POR0	-69.917	11.789	12.4	12.5	1.2	1.1	17.6
PRE0	-71.775	8.029	-4.2	12.5	1.2	1.0	13.2
QUI0	-69.646	9.871	6.1	16.5	1.2	1.0	17.6
SAR0	-70.001	12.180	13.4	11.0	1.5	1.3	17.3
TAL0	-71.681	7.801	-7.2	9.0	1.3	1.1	11.5
UMU0	-72.050	8.235	2.7	15.4	1.2	1.0	15.7
URI0	-71.743	7.913	-2.4	11.3	1.2	1.0	11.5
VAN0	-71.882	8.092	1.0	13.9	1.2	1.0	13.9
VIC0	-71.327	10.379	10.1	12.5	1.0	0.9	16.1
YAG0	-70.530	10.062	4.9	19.9	1.1	1.0	20.5
YER0	-69.108	11.345	12.7	15.9	1.2	1.1	20.3

(*) Stations in Colombia territory.

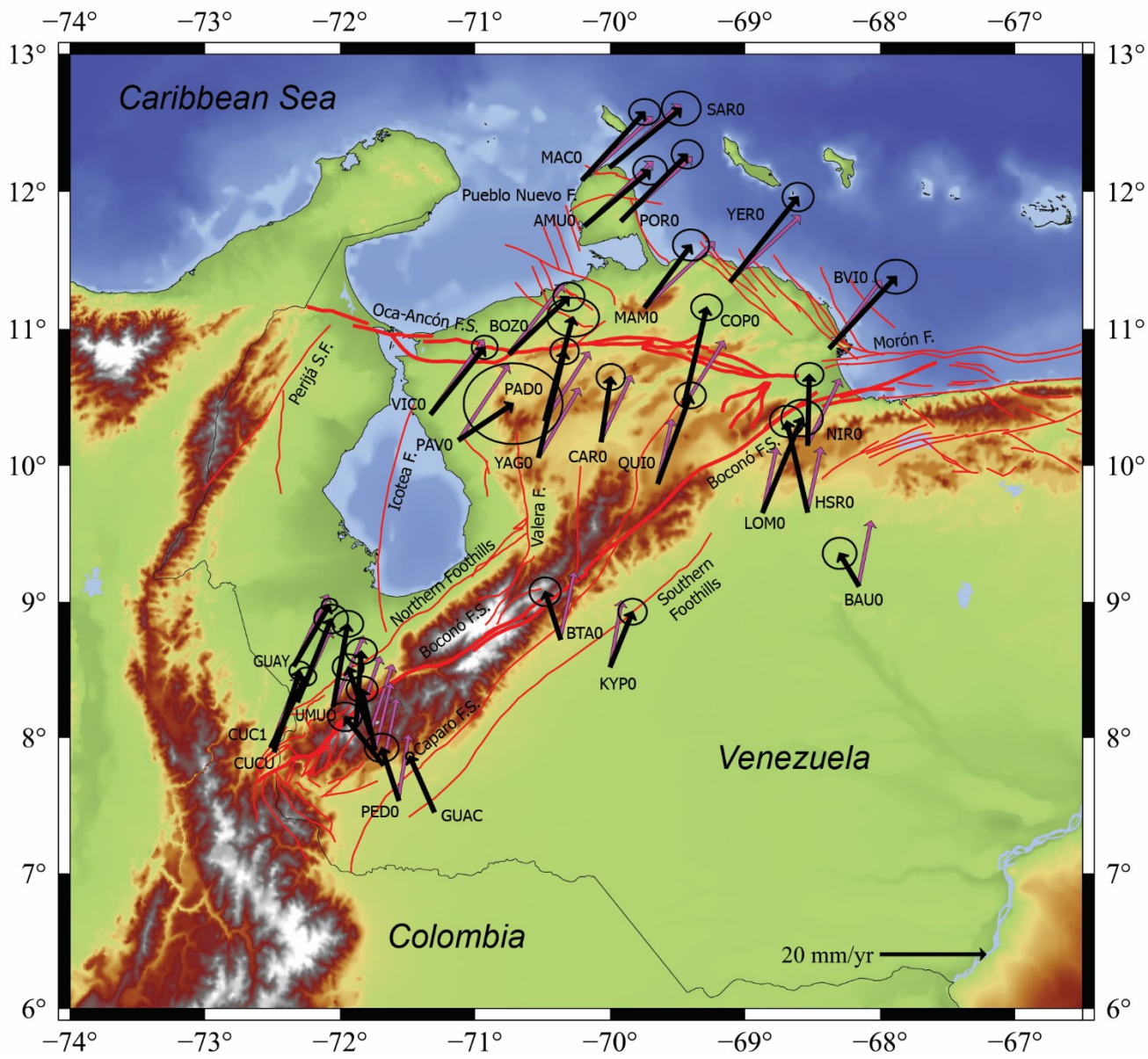

Figure 4. Velocities expressed in the ITRF2014 reference frame (black arrows) and velocities calculated in the surface deformation model VEMOS 2017 (magenta arrows). Quaternary fault map shown is from Audemard et al. (2000), and the relief map is from NOAA National Geophysical Data Center (2009).

3. GNSS VELOCITY FIELD

The velocity field across Western Venezuela exhibits several patterns. From velocities expressed in the ITRF2014 reference frame (Figure 4), we observe the sites on the northern side of the Oca-Ancon fault showing east and north components quite similar that result in velocities from 15 to 20 mm yr^{-1} with azimuth varying from 37° to 50°. In the known Trujillo Triangle, bounded by the Valera, Boconó, and Oca-Ancon faults, velocities show higher north component velocities than the stations located east of them, with resulting azimuth from 8.3° to 15°. PADO, YAGO, QUI0, and COPO sites are very similar except for the CAR0 site located in the center of Trujillo Triangle.

West of the Valera fault, on the Lake (Maracaibo) West Coast, the VIC0 and PAD0 sites show differences. However, the sigma error values of PAV0 are the highest of the whole dataset. The sites distributed to the southeast of the Boconó fault show a minor eastward-directed velocity component compared to the northward-directed component. The BAU0, HSR0, and NIR0 sites show a NW sense, while the LOM0, KYP0 sites are NE-directed. The BTA0 located in the Andean foothills also shows an arrow with NW sense. The rest of the sites localized in the

Southern Merida Andes seem to respond to this region's geological complexity.

The sites along the NW-SE trending profile extending from GUAY to GUAC show a counterclockwise variation of their azimuth from north to south. The GUAY site shows an azimuth of 30° that changes progressively to 342° for the PRE0 site. The URI0, TAL0, PED0, and GUAC sites show equal NW sense varying from 321° to 348°. The CUC1 and CUCU, two Colombian sites slightly westward of the profile, are similar to the Venezuelan GUAY and DAL0 sites located northeast of the 2 Colombian ones.

Figure 5 shows velocities referred to the South American Plate Reference Frame (Altamimi et al., 2017). The confirmation of some patterns of the previous figure is visualized. The entire assembly of stations north of the Oca-Ancon fault shows a dominant eastward component. According to previous studies, the magnitude and sense of velocity vectors are typical of the Caribbean Plate movement (e.g., Perez et al., 2001a; Reinoza, 2014; Mogollón-López et al., 2019; Molero, 2020).

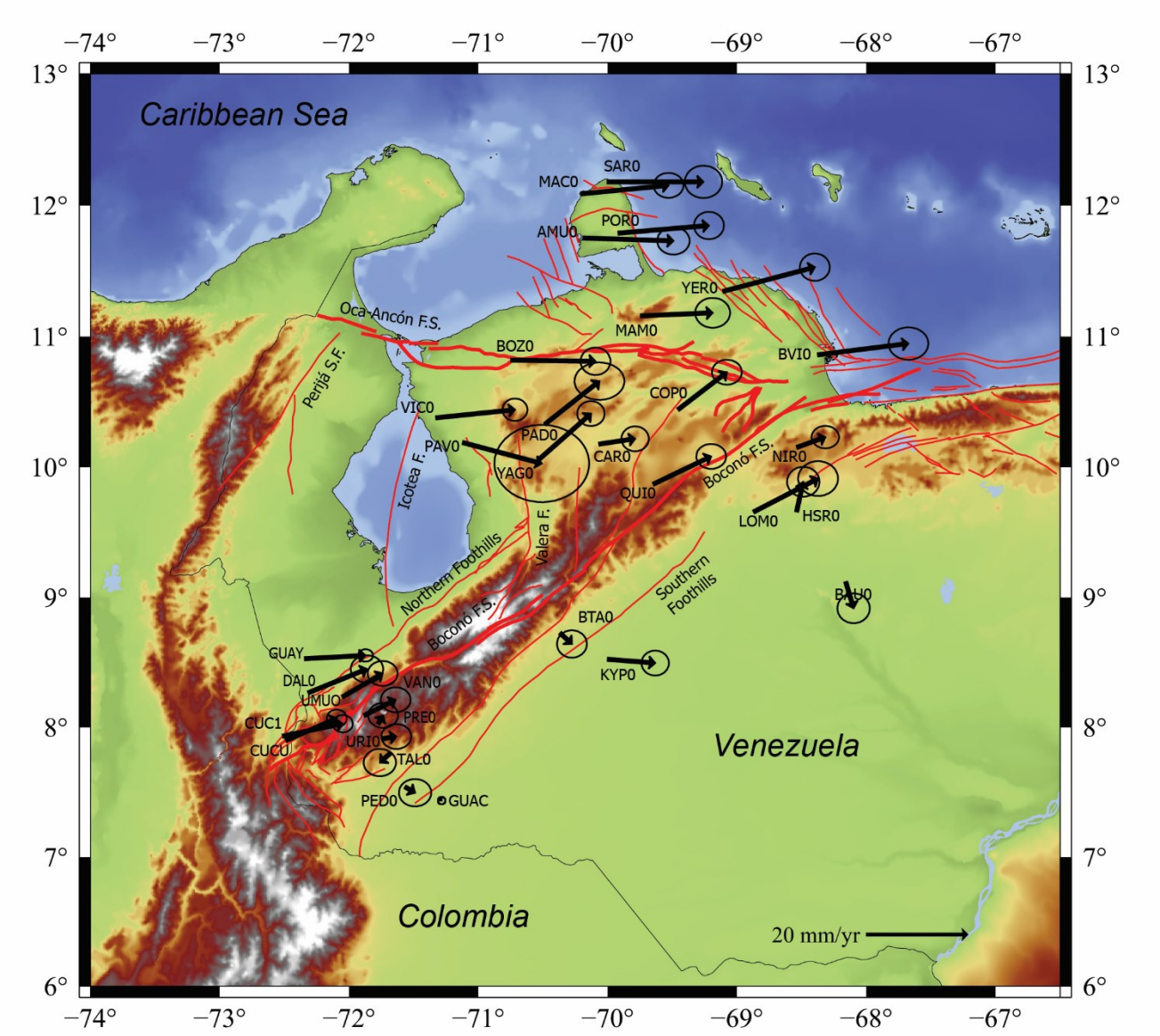

Figure 5. Observed velocities (black arrows) with ellipses for a 95% confidence level, reported on relief map from NOAA National Geophysical Data Center (2009) and Quaternary fault map shown is from Audemard et al. (2000). The displacements are expressed in the South America Plate Reference frame using the rotation pole proposed by Altamimi et al. (2017).

The velocities decrease in magnitude on the southern side of the Oca-Ancon fault, specifically in the Trujillo Triangular Block. However, the north component becomes more significant. The motion seems to show the typical NE escape direction of the Maracaibo Block, indicated by many previous works (e.g., Audemard, 1993, 1998, 2003, 2009; Audemard and Audemard, 2002; among many others), except for the PAV0 site that shows southeastward motion; however, as mentioned before this site has significant sigma errors.

Crossing the northern segment of the Boconó fault to the SE, we have found similarities in NE sense for LOM0 and NIR0 sites. We found a pattern for the BTA0, KYP0, and BAU0, with southeastward motion relative to stable South America, but the motion of HSR0 site concerning neighboring sites is unclear. In the southern region of the Merida Andes, we observe similarities in DAL0, UMUO, CUC1, and CUCU sites that show NE sense with azimuth varying from 60° to 78°. The GUAY site almost reaches the E-W sense. From VAN0 to the GUAC site, the velocities decrease in magnitude with an unexpected change to SW sense in the TAL0 site. Finally, PED0 and GUAC sites are shown with southeastward motion. All sites sitting southeast of the main relief of the Mérida Andes (BTA0, KYP0, PEDO, and GUAC; even BAU0), on the chain southern foothills and even on the western Venezuelan Llanos, clearly show consistent displacements towards the Guayana craton (to the southeast).

Comparison with VEMOS17

The present-day continuous surface-kinematic model for the entire Latin American and Caribbean region (VEMOS17) was calculated from geodetic velocities of 515 continuous sites. The observations were performed between January 01, 2014, and January 28, 2017, using a geodetic least-squares collocation approach with empirically determined covariance functions (Drewes and Sánchez, 2020). Unfortunately, the VEMOS17 model does not account for geodetic stations for our study area. However, it is the velocity model recommended by the Geodetic Reference System for the Americas (SIRGAS). For this reason, we find it relevant to compare the multi-year solution VEMOS17 with our GNSS observed velocities between 2011 and 2016 for western Venezuela to assess the adjustment of the model concerning several tectonic blocks. For such purpose, we calculated the velocity for each GNSS site based on the VEMOS17 through the finite element model and by a least squares collocation approach developed by Drewes and Heidbach (2012).

The most considerable differences between the surface deformation model of VEMOS17 (Sánchez and Drewes, 2020) and our velocities are observed in the BAU0, BTA0, COP0, HSR0, LOM0, PAD0, PAV0, QUI0, and YAG0 sites (Table 3). All these sites are located on the eastern part of the Maracaibo Block and the southeastern side of the Bocono Fault, towards the Baul Massif.

On the contrary, the sites located north of the Oca-Ancon Fault, in the Bonaire Block, and the sites on the southern Andes show more similarities between simulated (VEMOS17) and observed velocities (Figure 4). The highest arithmetic variation corresponds to the LOM0 station (Table 3); however, the BAU0 site on the Precambrian Baul Massif shows a significant percentage change in magnitude (Figure 4). Both sites are east of the Boconó fault and out of the Mérida Andes, on the South American plate.

Table 3. Differences between our velocities in comparison with VEMOS17.

Diff.	Ve (mm yr^{-1})	Vn (mm yr^{-1})	Speed (mm yr^{-1})
Max	5.87 (NIR0)	7.29 (PAV0)	6.81 (LOM0)
Min	0.03 (VIC0)	0.32 (CAR0)	0.19 (VAN0)
Mean	2.09	2.70	2.42
	Standard deviation		
	σVe (mm yr^{-1})	σVn (mm yr^{-1})	σSpeed (mm yr^{-1})
	2.57	3.53	3.09

4. ELASTIC MODELS ON THE SOUTHERN REGION OF THE MÉRIDA ANDES

Homogeneous elastic half-space model

The southern region of the Mérida Andes was selected to apply an elastic model because of the density of the positioned sites and their distribution following an approximately aligned profile transverse to known main structures (Figures 4 and 5). A first-order model of interseismic deformation (Chinnery, 1961; Weertman and Weertman, 1965; Savage and Burford, 1973) is represented by the relationship as follows (ec. 1),

$$V_{(X)} = \frac{V_T}{\pi}\tan^{-1}\left(\frac{X}{D}\right), \qquad (1)$$

where $V_{(x)}$ is the velocity at a distance X from the fault, V_T is the far-field velocity, and D is the locking depth of the fault. We first evaluate a first-order interseismic deformation model considering the southwestern segment of the Boconó fault (La Grita segment) alone, for which we evaluate four possibilities varying the number of sites (Figure 6). In the first test, we considered only the sites measured (PED0, TAL0, URI0, PRE0, VAN0, UMU0, and DAL0) by our team (V_T=13.0 mm yr^{-1} ; D=15.5 km). Next, we

include the Colombian CUCU and CUC1 sites (V_T =13.3 mm yr^{-1} ; D=14.8 km). In a third test, we add GUAY and GUAC measured by USB working group to the seven initial sites (V_T=10.7 mm yr^{-1}; D=12.9 km), and finally, we include all available sites (V_T=11.3 mm yr^{-1}; D=9.6 km). In the second part, we assess a two-fault model considering the Boconó and Caparo faults. We applied the same criterion of changing (increasing) the number of sites. The results are shown in Figure 7.

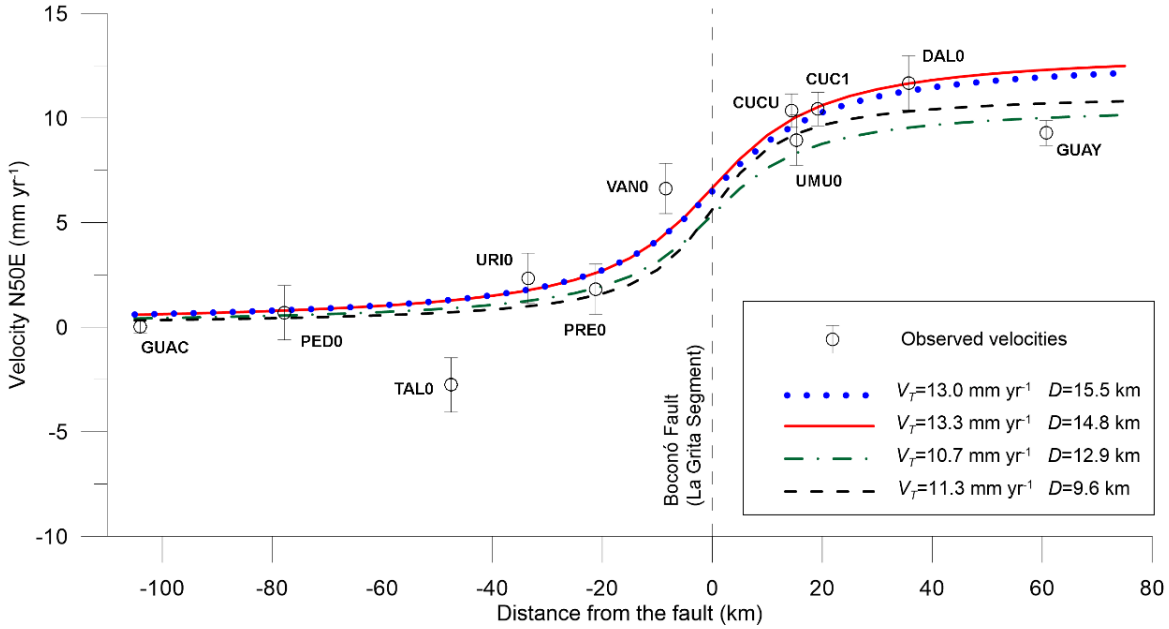

Figure 6. Across-fault velocity gradient using a homogeneous-simple model for a single fault. (Model 1: blue dots; Model 2: red solid line; Model 3: green dot dash line; Model 4: black dashed line).

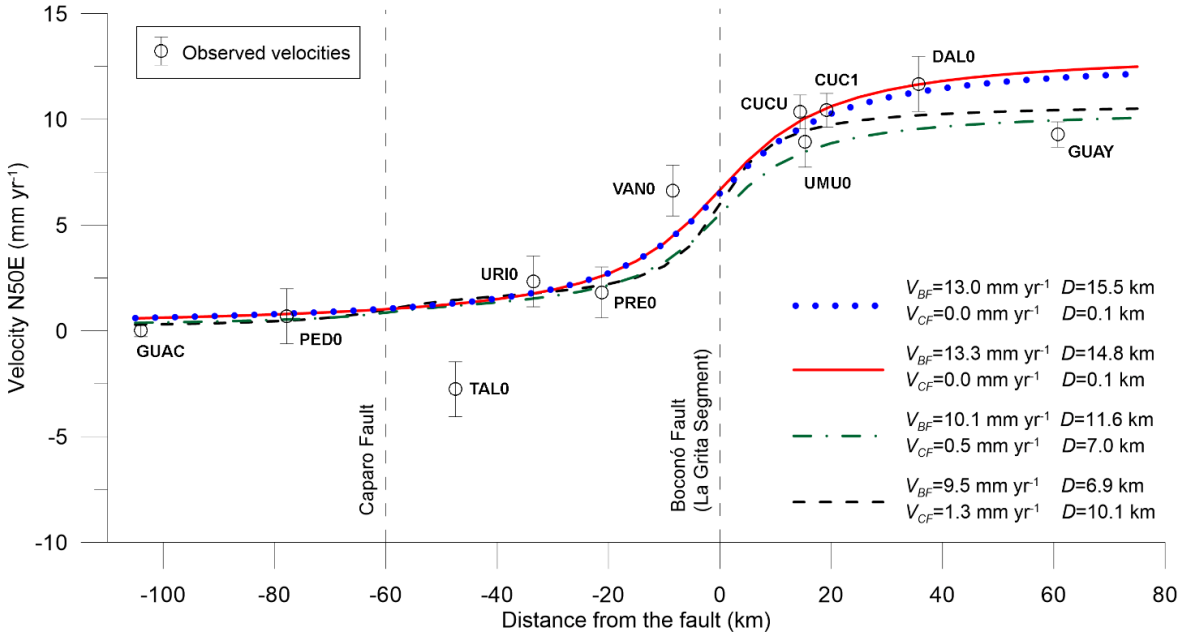

Figure 7. Across-fault velocity gradient for a two-fault model, considering the Caparo fault and the Boconó fault. (Model 5: blue dots; Model 6: red solid line; Model 7: green dot dash line; Model 8: black dashed line).

To evaluate the quality of our tests, we apply the Fisher-Snedecor test to select our preferred model (Table 4). First, we calculated an RMS or the quadratic mean value of the misfit for each possibility (ec.2) given by

$$RMS = \sqrt{\frac{1}{N}\sum\left(\frac{\left(V_{obs(X)} - V_{(X)}\right)^2}{\sigma^2_{V_{obs(X)}}}\right)}, \quad (2)$$

Where $\sigma^2_{V_{obs(X)}}$ is the variance of the observations, $V_{obs(X)}$ is the parallel component from observed interseismic velocities, $V_{(X)}$ is the simulated velocity at a distance X from the fault (ec.1), and N is the number of GNSS stations. Next, we determine the probability that one model is better than another. The Fisher-Snedecor test allows us to compare the single fault model to the two faults and select the most probable between these models.

From this comparison, the models considering all sites show better results in each category (one or two faults). However, model 4, including all sites and considering only the Boconó fault, is probably the best, with a far-field velocity of 11.3 mm yr^{-1} and a locking depth of 9.6 km. In general, the results of one-fault and two-fault models confirm that the Boconó fault is the main structure and, according to the best model, accounts for most of the slip allowing the tectonic escape of the North Andes Block or Sliver. In the next section, we carry out a comparison with geologically-derived slip rates (Table 5).

5. DISCUSSION AND CONCLUSIONS

The main outcome of the velocity field expressed in the ITRF2014 reference frame is the counterclockwise rotation of the slip vectors transverse to the Mérida Andes from northwest to southeast, from the GUAY to GUAC sites (Figure 4). We also identify some differentiated patterns in the Southern Venezuelan Andes (Figures 4 through 7) according to the observed velocities. However, the velocity field map relative to fixed South America (Figure 5) allows the distinction of at least three main clusters of sites. First, northwest of the Boconó Fault, several sites (CUCU, CUC1, DAL0, GUAY, and UMU0) show similar direction, magnitude, and sense of motion (Figures 4 through 7).

Second, immediately to the SE of the Boconó fault and northwest of the Uribante fault, we could group VAN0, PRE0, and URI0 sites. These intermediate sites would sit on a microblock that exhibits a considerable decrease in the vector magnitude relative to the immediate northern sites but keep a similar sense and direction. The third pattern is associated with PED0 and GUAC sites with southeastward motion, although the TAL0 site between these two sites shows an unexpected SW sense.

Table 4. Selection of preferred model according to Fisher-Snedecor variance test.

Model	N DATA	N parameters	Degree of freedom	RMS
One-fault modelling				
1 (7 sites)	7	2	5	1.429
2 (7s + CUC1, CUCU)	9	2	7	1.280
3 (7s + GUAC, GUAY)	9	2	7	1.573
4 (All sites)	11	2	9	1.610
Two-fault modeling				
5 (7 sites)	7	4	3	1.429
6 (7s + CUC1, CUCU)	9	4	5	1.280
7 (7s + GUAC, GUAY)	9	4	5	1.565
8 (All sites)	11	4	7	1.560
Comparison of models		Test (f value)	Probability (F ≤ f value)	Results
Is the 1 model better than the 2 model?		0.640	0.285	No
Is the 3 model better than the 2 model?		0.814	0.397	No
Is the 4 model better than the 2 model?		1.022	0.524	Maybe
Is the 5 model better than the 6 model?		0.537	0.256	No
Is the 6 model better than the 7 model?		1.223	0.584	Maybe
Is the 8 model better than the 6 model?		1.149	0.582	Maybe
Is the 4 model better than the 6 model?		1.246	0.629	Yes

Table 5. Geologically-derived slip rate for the southern region compared with our modeling approaches for 1- or 2- faults.

Fault name	Average slip rate (mm yr^{-1}) [a]	Sense of movement	Slip rate (mm yr^{-1}) from	
			1 Fault M.	2 Fault M.
Northern Foothills	0.5	Reverse		
Aguas Calientes-San Simón	1.5-1.0	Right lateral – reverse (H>V)		
Boconó (La Grita segment)	5.2±0.9	Right lateral	11.3	9.5
Uribante	0.5	Right lateral – normal (H>V)		
Central Andean System (North, South)	0.4	Normal – Right lateral (V>H)		
Caparo (West, East)	2.5-0.9	Right lateral		1.3
Southern Foothills	0.5	Reverse		

[a] Slip rates from (Audemard et al., 2000; Audemard, 2001 and references therein; Paolini et al., 2012)

These two sites (PED0 and GUAC) on the southern Mérida Andes show a similar motion behavior to the other sites sitting further northeast but also outside the main body of this Mérida Andes (BTA0 and KYP0) and on its southern foothills or very close; even with BAU0 (Baul Massif), which is frankly off the Andes and south of the mostly Eocene-emplaced Cordillera de La Costa Nappes system.

These four sites (PED0, GUAC, BTA0, and KYP0), along with BAU0, display a Guayana Shield-directed displacement (Figure 5), which would suggest that shortening is the main tectonic process in the southeastern half of the Mérida Andes, as well as in the southern edge of the nappes system. It seems to support the strain partitioning proposed by Audemard and Audemard (2002) for the Mérida Andes, based mainly on instrumental seismicity and the proposed subsurface geometry under this chain by these authors: across-chain shortening (convergence) in NW-SE direction, occurring mainly within the brittle crust over a low angle NW-dipping detachment corresponding to the brittle-ductile transition, under which the South American plate is incipiently subducting (continental subduction) or underthrusting, while the Boconó fault takes dextral slip and concomitantly allows the NNE-directed tectonic escape of the Triangular Maracaibo block.

Assuming that this tectonic model happens to be correct, both shortening and NE-directed dextral slip must occur on structures (jointly or separately) in the northern half of the Mérida Andes (north of Boconó fault), which also appears to be supported by the displacement field here derived (Figures 4 and 5).

A good correlation exists in the Southern Venezuelan Andes on the northern side of the Boconó fault between the ITRF2014 velocities map and VEMOS17 (Figure 4). To the south, we may see the transition between the South American and Caribbean plates crossing this complex-wide deformation zone. VAN0, PRE0, URI0, TAL0, PED0, and GUAC sites show a transition zone that is not shown in the big-scale deformation models. In the Venezuelan case, VEMOS17 is presented as an option for the correction by epoch stations of the Venezuelan Geocentric Network (REGVEN), which is referred to as the ITRF94 epoch 1995.4.

However, the differences in magnitude and direction of the velocity vectors confirm that this model cannot reproduce regional and local phenomena due to the lack of data in areas with seismic activity in Venezuela. The multi-year solution SIR17P01 used by SIRGAS to calculate VEMOS17, spanning from April 17, 2014, to January 28, 2017, comprises three episodic GPS campaigns. Also, this solution comprised only data for three sites in Venezuela (MARA, CRCS, CUM3) located in the northern continental part of the country, on the rooftops of buildings and two monuments over metallic towers. These siting configurations increase the uncertainty in the calculated velocity because the impact of man-made-structure deformation was not computed in the results.

The data used for the solution covered from April 04, 2011, to the first trimester of 2014, when, unfortunately, they were ruled out from SIRGAS solution computation due to non-compliance with the standards and conventions of the IERS (International Earth Rotation and Reference Systems Service) and IGS (Cioce et al., 2015). In addition, these three original stations are also distanced 200 km apart, affecting the colocation methods to correlate velocities based on the long distance between stations.

A quick glance at the active tectonics of western Venezuela (e.g., Audemard et al., 2000; Audemard and Audemard, 2002) shows remarkable structures such as the Maracaibo block, Merida Andes, and Llanos Basins, and active geologic faults like the Oca-Ancón, Valera, and Boconó fault, among others. The Boconó fault is a strike-slip fault that extends for over 500 km and is segmented into five sections according to geometric criteria (Audemard, 2014b).

The design of our geodetic network (mainly an across-chain profile) only crosses the La Grita segment with sufficient detail, which extends from the proximity to the Colombian border (Mirtos pull-apart basin) to the Lagunillas pull-apart basin. It seems clear that improving and densifying the geodetic network is necessary. Concerning a simple homogeneous model for the Boconó fault in the southern region of the Mérida Andes, the observed and modeled velocities show a reasonable agreement (Figures 6, 7).

We have found significant difficulties in simulating the velocities of TAL0 site with the homogeneous elastic half-space model. A future observation campaign may help constrain this motion's source and determine if it responds to tectonic processes or other causes. For this study, we are not considering convergence across adjacent and subparallel thrust faults.

The slip rates obtained in the simple homogeneous models are present-day dislocation-in-depth. For this reason, it is difficult to compare these slip rates with the geologically derived slip rates for the southern region (Table 5). In a brief analysis, we compare DAL0 and UMU0 displacements (Fig. 5), finding a velocity gradient of 2.7 mm yr^{-1} on the surface through the right-lateral Aguas Calientes-San Simón fault, a value coherent with 1.0-1.5 mm yr^{-1} of Table 5. The comparison between URI0 and PED0 velocities shows a gradient of 1.6 mm yr^{-1} through the Uribante and Caparo fault system.

This result is consistent with the arithmetic sum of the individual geologically derived slip rates for the Uribante and Caparo fault (1.4-3.0 mm yr^{-1}). Likewise, the velocity gradient between DAL0 and PED0 sites (Figure 6), which are separated by Aguas Calientes-San Simón, Boconó, Uribante and Caparo faults (Figure 2), is in the order of 10 mm yr^{-1}, which is similar to the simple addition (6.7-10.6 mm yr^{-1}) of the individual geologic slip rates of Aguas Calientes (1.0-1.5 mm yr^{-1}) and Boconó (5.2±0.9 mm yr^{-1} at La Grita segment; Audemard, 1997), Uribante (5 mm yr^{-1}), and Caparo (0.9-2.5 mm yr^{-1}) faults (Table 5).

This added geodetic slip rate of >10 mm yr^{-1}, from these four major faults running along and within the Mérida Andes from NW to SE is the same as the slip rate proposed by Audemard et al., 1999, 2008) for the Boconó segments extending between Mérida and Boconó (Boc-b –o la Grita- and Boc-c, after Audemard, 2014b), estimated at the lake Mucubají pass, at the releasing stepover bounding the Apartaderos pull-apart basin, and is comparable to the geodetic slip rate of 11.3 mm yr^{-1} (model 4).

DECLARATION OF CONFLICT OF INTEREST

The authors declare that the article does not present a conflict of interest.

ACKNOWLEDGMENTS

The geodesic measurements were carried out with personnel and equipment of FUNVISIS (Alexi Suarez, Antonio Dasco, Javier Oropeza, Jélime Aray, Ricardo López, Osmar Zambrano, Victor Rocabado, Sirel Colón), PDVSA (Abdenago Nahmens, Carlos Mijares, Dionicio Montero, Emiliano Morón, Joe Angarita, Reny Espinosa, Tomás Solarte, Yeldy Molero), PDVSA-INTEVEP (Carlos Martínez, Luis Martínez, Manuel Rondón, Pedro Medina, Ramón Gómez, Yeraldine Rivera), and IGVSB (Eliezer Concha, Yohana Bautista). We especially thank those who collaborated in the reconnaissance, installation, and measurement campaigns. Thanks to Dr. Luz María Rodríguez (FUNVISIS) for helping us compile historical seismicity. This research is a contribution to FONACIT-2013000361 (Tsunami), FONACIT-2012002202 (GIAME), and PI-641189 (CICESE). Map figures (3, 4, and 7) were generated by the Generic Mapping Tool (GMT) software (Wessel et al., 2013). The authors thank two anonymous reviewers and the Editor Mario Maya for their helpful comments and suggestions.

REFERENCES

Altamimi, Z., Métivier, L., Rebischung, P., Rouby, H., & Collilieux, X. (2017). ITRF2014 plate motion model. Geophysical Journal International, 209(3), 1906–1912. https://doi.org/10.1093/gji/ggx136

Audemard, F. A. (1993). Néotectonique, sismotectonique et aléa sismique du nord-ouest du Vénézuela (système de failles d'Oca-Ancón).

Audemard, F. A. (1997). Holocene and historical earthquakes on the Boconó fault system, southern Venezuelan Andes: Trench

confirmation. Journal of Geodynamics, 24(1), 155–167. https://doi.org/https://doi.org/10.1016/S0264-3707(96)00037-3

Audemard, F. A. (1998). Evolution géodynamique de la facade nord Sud-américaine: nouveaux apports de l'histoire geéologique du Bassin de Falcón, Vénézuéla. XIV Caribbean Geological Conference, 2, 327–340.

Audemard, F. A. (2001). Revisión y actualización de los parámetros sismogénicos de las fallas activas o potencialmente activas en Venezuela (Parcial Rpt. to Project INTEVEP 99-162). FUNVISIS' Unpublished Rpt for INTEVEP S.A, 24 pp + appendices.

Audemard, F. A. (2003). Geomorphic and geologic evidence of ongoing uplift and deformation in the Mérida Andes, Venezuela. Quaternary International, 101–102, 43–65. https://doi.org/https://doi.org/10.1016/S1040-6182(02)00128-3

Audemard, F. A. (2009). Key issues on the post-Mesozoic Southern Caribbean Plate boundary. Geological Society, London, Special Publications, 328(1), 569. http://sp.lyellcollection.org/content/328/1/569.abstract

Audemard, F. A. (2014a). Active block tectonics in and around the Caribbean: A review. In M. Schmitz, F. Audemard, & F. Urbani (Eds.), El Límite Noreste de la Placa Suramericana – Estructuras Litosféricas de la Superficie al Manto (pp. 29–77). Universidad Central de Venezuela y FUNVISIS.

Audemard, F. A. (2014b). Segmentación sismogenética de la falla de Boconó a partir de investigaciones paleosísmicas por trincheras, Venezuela occidental: ¿migración de la ruptura hacia el noreste en tiempos históricos? Revista de La Asociación Geológica Argentina, 71(2), 247–259.

Audemard, F. A., Machette, M. N., Cox, J. W., Dart, R. L., & Haller, K. M. (2000). Map of Quaternary Faults of Venezuela. USGS Open-File Report 00-0018. http://greenwood.cr.usgs.gov/pub/open-file-reports/ofr-00-0018

Audemard, F. A., Ollarves, R., Bechtold, M., Díaz, G., Beck, C., Carrillo, E., Pantosti, D., & Diederix, H. (2008). Trench investigation on the main strand of the Boconó fault in its central section, at Mesa del Caballo, Mérida Andes, Venezuela. Tectonophysics, 459(1), 38–53. https://doi.org/https://doi.org/10.1016/j.tecto.2007.08.020

Audemard, F. A., Reinoza, C., López, R., Feaux, K. & Jouanne, F. (2020). Instalación de estaciones geodésicas de monitoreo continuo para fines geocientíficos en el margen caribe sureste. Boletín de Geología, 42(2). https://doi.org/10.18273/revbol.v42n2-2020001.

Audemard, F. A., Romero, G., Rendon, H., & Cano, V. (2005). Quaternary fault kinematics and stress tensors along the southern Caribbean from fault-slip data and focal mechanism solutions. Earth-Science Reviews, 69(3–4), 181–233. https://doi.org/10.1016/j.earscirev.2004.08.001.

Audemard, F. E., & Audemard, F. A. (2002). Structure of the Mérida Andes, Venezuela; relations with the South America-Caribbean geodynamic interaction. Tectonophysics, 345(1–4), 299–327.

Audemard, F. E., Pantosti, D., Machette, M., Costa, C., Okumura, K., Cowan, H., Diederix, H., & Ferrer, C. (1999). Trench investigation along the Mérida section of the Boconó fault (central Venezuelan Andes), Venezuela. Tectonophysics, 308(1), 1–21. https://doi.org/https://doi.org/10.1016/S0040-1951(99)00085-2

Ávila-Barrientos, L., Cabral-Cano, E., Nava Pichardo, F. A., Reinoza, C. E., Salazar-Tlaczani, L., & Fernández-Torres, E. (2021). Surface deformation of Ceboruco volcano, Nayarit, Mexico. Journal of Volcanology and Geothermal Research, 418, 107338. https://doi.org/https://doi.org/10.1016/j.jvolgeores.2021.107338

Avila-García, J., Schmitz, M., Mortera-Gutierrez, C., Bandy, W., Yegres, L., Zelt, C., & Aray-Castellano, J. (2022). Crustal structure and tectonic implications of the southernmost Merida Andes, Venezuela, from wide-angle seismic data analysis. Journal of South American Earth Sciences, 116, 103853. https://doi.org/https://doi.org/10.1016/j.jsames.2022.103853

Backé, G., Dhont, D., & Hervouët, Y. (2006). Spatial and temporal relationships between compression, strike-slip and extension in the Central Venezuelan Andes: Clues for Plio-Quaternary tectonic escape. Tectonophysics, 425(1), 25–53. https://doi.org/https://doi.org/10.1016/j.tecto.2006.06.005

Bezada, M. J., Magnani, M. B., Zelt, C. A., Schmitz, M., & Levander, A. (2010). The Caribbean-South American plate boundary at 65°W: Results from wide-angle seismic data. J. Geophys. Res., 115(B8), B08402. https://doi.org/10.1029/2009jb007070

Chinnery, M. A. (1961). The deformation of the ground around surface faults. Bulletin of the Seismological Society of America, 51(3), 355–372. http://www.bssaonline.org/content/51/3/355.abstract

Cioce, V., Rincón, M. F., Wildermann, E., Royero, G., Reinoza, C., Audemard, F. A., & Sánchez, L. (2015). Una alternativa para el mantenimiento del marco de referencia SIRGAS en Venezuela. Simposio Sistema de Referencia Geocéntrico Para Las Américas SIRGAS.

Coates, A. G., Collins, L. S., Aubry, M.-P., & Berggren, W. A. (2004). The Geology of the Darien, Panama, and the late Miocene-Pliocene collision of the Panama arc with northwestern South America. Geological Society of America Bulletin, 116(11–12), 1327–1344. https://doi.org/10.1130/B25275.1

Colmenares, L., & Zoback, M. D. (2003). Stress field and seismotectonics of northern South America. Geology, 31(8), 721–724. https://doi.org/10.1130/g19409.1

Cifuentes, H., & Sarabia, A. (2007). Estudio macrosísmico del sismo del 16 de enero de 1644, Pamplona (Norte de Santander). https://sish.sgc.gov.co/visor/sesionServlet?metodo=irAInfoDetallada&idSismo=22#

Dach, R., & Fridez, P. (2019). Bernese GNSS Software Version 5.2, Tutorial Processing Example Introductory Course Terminal Session. Astronomical Institute, University of Bern.

Dach, R., Lutz, S., Walser, P., & Fridez, P. (Eds.). (2015). Bernese GNSS Software Version 5.2. University of Bern, Bern Open Publishing Text. https://doi.org/10.7892/boris.72297

Dhont, D., Backé, G., & Hervouët, Y. (2005). Plio-Quaternary extension in the Venezuelan Andes: Mapping from SAR JERS imagery. Tectonophysics, 399(1–4), 293–312. https://doi.org/10.1016/j.tecto.2004.12.027

Drewes, H., & Heidbach, O. (2012). The 2009 Horizontal Velocity Field for South America and the Caribbean. In S. Kenyon, M. C. Pacino, & U. Marti (Eds.), Geodesy for Planet Earth (pp. 657–664). Springer Berlin Heidelberg.

Drewes, H., & Sánchez, L. (2020). Velocity model for SIRGAS 2017: VEMOS2017. PANGAEA. https://doi.org/10.1594/PANGAEA.912350

Duque-Caro, H. (1979). Major Structural Elements and Evolution of Northwestern Colombia. In Geological and Geophysical Investigations of Continental Margins. American Association of Petroleum Geologists. https://doi.org/10.1306/M29405C22

Egbue, O., & Kellogg, J. (2010). Pleistocene to Present North Andean "escape." Tectonophysics, 489(1–4), 248–257. https://doi.org/http://dx.doi.org/10.1016/j.tecto.2010.04.021

Galán, R. A., & Casallas, I. F. (2010). Determination of effective elastic thickness of the Colombian Andes using satellite-derived gravity data. Earth Sciences Research Journal, 14(1), 7–16.

Galan, R., Gómez, A., Sarabia, A. M., Sanchez, V., Rodriguez, L., & Santulin, M. (2016). Calculo de parametros fisicos del terremoto de Cucuta de 1875 a partir de intensidades macrosismicas actualizadas. Regional Assembly Latin American and Caribbean Seismological Commision, IASPEI.

Gutscher, M.-A., Spakman, W., Bijwaard, H., & Engdahl, E. R. (2000). Geodynamics of flat subduction: Seismicity and tomographic constraints from the Andean margin. Tectonics, 19(5), 814–833. https://doi.org/10.1029/1999TC001152

Hugentobler, U., Schaer, S., Fridez, P., Beutler, G., Bock, H., Brockmann, E., Dach, R., Gurtner, W., Ineichen, D., Johnson, J., & others. (2001). Bernese GPS software, version 4.2.

Jarrin, P., Nocquet, J.-M., Rolandone, F., Audin, L., Mora-Páez, H., Alvarado, A., Mothes, P., Audemard, F., Villegas-Lanza, J. C., & Cisneros, D. (2023). Continental block motion in the Northern Andes from GPS measurements. Geophysical Journal International, 235(2), 1434–1464. https://doi.org/10.1093/gji/ggad294

Johnston, G., Riddell, A., & Hausler, G. (2017). Springer Handbook of Global Navigation Satellite Systems (P. J. G. Teunissen & O. Montenbruck, Eds.). Springer International Publishing. https://doi.org/10.1007/978-3-319-42928-1

Jouanne, F., Audemard, F. A., Beck, C., Van Welden, A., Ollarves, R., & Reinoza, C. (2011). Present-day deformation along the El Pilar Fault in eastern Venezuela: Evidence of creep along a major transform boundary. Journal of Geodynamics, 51(5), 398–410. https://doi.org/http://dx.doi.org/10.1016/j.jog.2010.11.003

Kellogg, J. N. (1984). Cenozoic tectonic history of the Sierra de Perija, Venezuela-Colombia, and adjacent basins. Geological Society of America Memoir, 162, 239–261.

Kellogg, J. N., & Bonini, W. E. (1982). Subduction of the Caribbean plate and basement uplifts in the overriding South American plate. Tectonics, 1(3), 251–276.

Kellogg, J. N., & Dixon, T. H. (1990). Central and South America GPS geodesy - CASA Uno. Geophysical Research Letters, 17(3), 195–198. https://doi.org/https://doi.org/10.1029/GL017i003p00195

Ladd, J. W., Truchan, M., Talwani, M., Stoffa, P. L., Buhl, P., Houtz, R., Maufiret, A., & Westbrook, G. (1984). Seismic reflection profiles across the southern margin of the Caribbean. In W. E. Bonini, R. B. Hargraves, & R. Shagam (Eds.), The Caribbean-South American Plate Boundary and Regional Tectonics (Vol. 162, p. 0). Geological Society of America. https://doi.org/10.1130/MEM162-p153

Lizarazo, S. C., Sagiya, T., & Mora-Páez, H. (2021). Interplate coupling along the Caribbean coast of Colombia and its implications for seismic/tsunami hazards. Journal of South American Earth Sciences, 110, 103332. https://doi.org/https://doi.org/10.1016/j.jsames.2021.103332

Malavé, G., & Suárez, G. (1995). Intermediate-depth seismicity in northern Colombia and western Venezuela and its relationship to Caribbean plate subduction. Tectonics, 14, 617–628. https://doi.org/10.1029/95tc00334

Mann, P., Burke, K., & Matumoto, T. (1984). Neotectonics of Hispaniola: plate motion, sedimentation, and seismicity at a restraining bend. Earth and Planetary Science Letters, 70(2), 311–324. http://www.sciencedirect.com/science/article/B6V61-472CFPT-2P/2/dfaf91a072f341231198136de17f1712

Mann, P., Schubert, C., & Burke, K. (1991). Review of Caribbean neotectonics. In The Caribbean Region (pp. 307–338). Geological Society of America. https://doi.org/10.1130/DNAG-GNA-H.307

McGeary, S., Nur, A., & Ben-Avraham, Z. (1985). Spatial gaps in arc volcanism: The effect of collision or subduction of oceanic plateaus. Tectonophysics, 119(1–4), 195–221. https://doi.org/http://dx.doi.org/10.1016/0040-1951(85)90039-3

Mogollón-López, J. A., Reinoza, C., Audemard, F. A., & Molero, Y. (2019). Análisis de la deformación inter-sísmica en el occidente venezolano a partir de datos GNSS. Revista de La Facultad de Ingeniería U.C.V., 34(2).

Molero, Y. (2020). Estudio geodinámico de los Andes de Mérida a partir de mediciones geodésicas GNSS. Universidad Simón Bolívar.

Molnar, P., & Sykes, L. R. (1969). Tectonics of the Caribbean and middle America regions from focal mechanisms and seismicity. Geological Society of America Bulletin, 80, 1639– 1684.

Müller, R. D., Royer, J.-Y., Cande, S. C., Roest, W. R., & Maschenkov, S. (1999). Chapter 2 New constraints on the late cretaceous/tertiary plate tectonic evolution of the caribbean (pp. 33–59). https://doi.org/10.1016/S1874-5997(99)80036-7

NOAA National Geophysical Data Center. (2009). ETOPO1 1 Arc-Minute Global Relief Model. NOAA National Centers for Environmental Information. https://www.ncei.noaa.gov/access/metadata/landing-page/bin/iso?id=gov.noaa.ngdc.mgg.dem:316

Palme, C., Aranguren, R., Leal, A., Choy, J., & Guada, C. (2012). Comentarios acerca del terremoto de La Grita 03/02/1610. VI Jornadas Venezolanas de Sismología Histórica.

Palme, C., Morandi S., M. T., & Choy, J. E. (2005). Determinación de una relación lineal entre intensidad, magnitud y distancia epicentral para el occidente de Venezuela. Interciencia,30,195–204.

Paolini, M., Rodríguez, L. M., & Olbrich, F. (2012). Actualización de las Fallas Activas de Venezuela como aporte a la evaluación de la

Amenaza Sísmica.

Pennington, W. D. (1981). Subduction of the Eastern Panama Basin and Seismotectonics of Northwestern South America. J Geophys Res, 86. https://doi.org/10.1029/JB086iB11p10753

Pérez, O. J., Bilham, R., Bendick, R., Hernández, N., Hoyer, M., Velandia, J. R., Moncayo, C., & Kozuch, M. (2001a). Velocidad relativa entre las placas del caribe y suramérica a partir de observaciones dentro del sistema de posicionamiento global (GPS) en el norte de Venezuela. Interciencia, 26(2), 69–74. https://www.redalyc.org/articulo.oa?id=33905305

Pérez, O. J., Bilham, R., Bendick, R., Velandía, J. R., Hernández, N., Moncayo, C., Hoyer, M., & Kozuch, M. (2001b). Velocity Field Across the Southern Caribbean Plate Boundary and Estimates of Caribbean/South-American Plate Motion Using GPS Geodesy 1994-2000. Geophys Res Lett, 28. https://doi.org/10.1029/2001gl013183

Pérez, O. J., Bilham, R., Sequera, M., Molina, L., Gavotti, P., Codallo, H., Moncayo, C., Rodríguez, C., Velandia, R., Guzmán, M., & Molnar, P. (2011). Campo de Velocidades GPS en el Occidente de Venezuela: Componente Lateral Derecha asociada a la falla de Boconó y Componente Convergente perpendicular a Los Andes. Interciencia, 36(1), 39–44.

Pérez, O. J., Wesnousky, S. G., De La Rosa, R., Márquez, J., Uzcátegui, R., Quintero, C., Liberal, L., Mora-Páez, H., & Szeliga, W. (2018). On the interaction of the North Andes plate with the Caribbean and South American plates in northwestern South America from GPS geodesy and seismic data. Geophysical Journal International, 214(3), 1986–2001. https://doi.org/10.1093/gji/ggy230

Pindell, J. L., & Barrett, S. F. (1990). Geologic evolution of the Caribbean: A plate-tectonic perspective. In G. Dengo & J. E. Case (Eds.), The Geology of North America. Vol, The Caribbean Region: Vol. H (pp. 405–432). Geological Society of America.

Pindell, J. L., & Dewey, J. F. (1982). Permo-Triassic reconstruction of western Pangea and the evolution of the Gulf of Mexico/Caribbeanregion. Tectonics, 1. https://doi.org/10.1029/TC001i002p00179

Pousse-Beltran, L., Vassallo, R., Audemard, F., Jouanne, F., Carcaillet, J., Pathier, E., & Volat, M. (2017). Pleistocene slip rates on the Boconó fault along the North Andean Block plate boundary, Venezuela. Tectonics, 36(7), 1207–1231. https://doi.org/10.1002/2016TC004305

Ramírez, J. E. (1953). El terremoto de Arboledas, Cucutilla y Salazar de Las Palmas, 8 de julio, 1950. Instituto Geofísico de los Andes Colombianos. https://books.google.com.mx/books?id=KxO0AAAAIAAJ

Reinoza Gómez, C. E. (2014). High resolution geodetic GNSS surveys of the present-day deformation along the South-Caribbean margin. Implications for earthquake hazard assessment in western and north-eastern Venezuela (Issue 2014GRENU041) [Université de Grenoble Alpes]. https://tel.archives-ouvertes.fr/tel-01230076

Reinoza, Gómez, C.E., Jouanne, F., Audemard, F. A., Schmitz, M., & Beck, C. (2015). Geodetic exploration of strain along the El Pilar Fault in northeastern Venezuela. Journal of Geophysical Research: Solid Earth, 120(3), 2014JB011483. https://doi.org/10.1002/2014JB011483

Reinoza-Gómez, C. E. (2015). Geodesy and Geodynamics. Bol. Acad. C. Fís., Mat. y Nat., LXXV(1), 43–54.

Salcedo-Hurtado, E. de J., Audemard, F. A., & García-Millán, N. (2021). Parámetros focales del terremoto del 28 de abril de 1894 en los Andes venezolanos usando datos macrosísmicos. Revista de La Academia Colombiana de Ciencias Exactas, Físicas y Naturales, 45(175), 591–606. https://doi.org/10.18257/raccefyn.1195

Sánchez, L., & Drewes, H. (2020). Geodetic Monitoring of the Variable Surface Deformation in Latin America. In International Association of Geodesy Symposia (pp. 1–12). Springer Berlin Heidelberg. https://doi.org/10.1007/1345_2020_91

Savage, J. C., & Burford, R. O. (1973). Geodetic determination of relative plate motion in central California. Journal of Geophysical Research (1896-1977), 78(5), 832–845. https://doi.org/10.1029/JB078i005p00832

Silver, E. A., Case, J. E., & Macgillavry, H. J. (1975). Geophysical Study of the Venezuelan Borderland. GSA Bulletin, 86(2), 213–226. https://doi.org/10.1130/0016-7606(1975)86<213:GSOTVB>2.0.CO;2

Singer, A., & Beltran, C. (1996). Active faulting in the southern Venezuelan Andes and Colombian Borderland. In Géodynamique andine : résumés étendus = Andean geodynamics : extended abstracts (pp. 243–246). ORSTOM. https://www.documentation.ird.fr/hor/fdi:010008569

Stephan, J. F., Lepinay, B. M. de, Calais, E., M. Tardy, Beck, C., J.C. Carfantan, Olivet, J. L., Vila, J. M., Bouysse, P., A.Mauffret, Bourgois, J., Thery, J. M., Tournon, J., Blancher, R., & Dercourt, J. (1990). Paleogeodynamic maps of the Caribbean: 14 steps from Lias to Present. Bulletin de La Société Géologique de France, 8, 915–919.

Symithe, S., Calais, E., Chabalier, J. B., Robertson, R., & Higgins, M. (2015). Current block motions and strain accumulation on active faults in the Caribbean. Journal of Geophysical Research: Solid Earth, 120(5), 3748–3774. https://doi.org/10.1002/2014JB011779

Taboada, A., Rivera, L. A., Fuenzalida, A., Cisternas, A., Philip, H., Bijwaard, H., Olaya, J., & Rivera, C. (2000). Geodynamics of the northern Andes: Subductions and intracontinental deformation (Colombia). Tectonics, 19, 787–813. https://doi.org/10.1029/2000tc900004

Trenkamp, R., Kellogg, J. N., Freymueller, J. T., & Mora, H. P. (2002). Wide plate margin deformation, southern Central America and northwestern South America, CASA GPS observations. Journal of South American Earth Sciences, 15(2), 157–171. http://www.sciencedirect.com/science/article/B6VDS-45D14NM-3/2/8990e29290c2fb6e0096ab0052c70454

Trenkamp, R., Kellogg, J. N., Mora, H., Freymueller, T., Dixon, T., & Leffer, L. (1995). Active Panama arc, northern Andes collision, GPS displacement vectors 1988-1994. Transactions, American Geophysical Union, 1995 Fall Meeting, 613.

Van der Hilst, R. van der, & Mann, P. (1994). Tectonic implications of tomographic images of subducted lithosphere beneath northwestern South America. Geology, 22(5), 451–454.

https://doi.org/10.1130/0091-7613(1994)022<0451:TIO-TIO>2.3.CO;2

Weber, J. C., Dixon, T. H., DeMets, C., Ambeh, W. B., Jansma, P., Mattioli, G., Saleh, J., Sella, G., Bilham, R., & Perez, O. (2001). GPS estimate of relative motion between the Caribbean and South American plates, and geologic implications for Trinidad and Venezuela. Geology, 29(1), 75-a-78. https://doi.org/10.1130/0091-7613

Weertman, J., & Weertman, J. R. (1965). Elementary Dislocation Theory. Macmillan Co.

Wessel, P., Smith, W. H. F., Scharroo, R., Luis, J., & Wobbe, F. (2013). Generic Mapping Tools: Improved Version Released. Eos, Transactions American Geophysical Union, 94(45), 409–410. https://doi.org/10.1002/2013EO450001